DFT Study of Oxygen Adsorption on Modified Nanostructured Gold Pyramids

5 AUTHORS, INCLUDING:

Frederik Tielens
Collège de France
93 PUBLICATIONS   1,329 CITATIONS

SEE PROFILE

Claudine Buess-Herman
Université Libre de Bruxelles
86 PUBLICATIONS   1,357 CITATIONS

SEE PROFILE

Paul Geerlings
Vrije Universiteit Brussel
452 PUBLICATIONS   11,545 CITATIONS

SEE PROFILE

ARTICLES

DFT Study of Oxygen Adsorption on Modified Nanostructured Gold Pyramids

F. Tielens and J. Andrés*

Departament de Ciències Experimentals, Box 224, Universitat Jaume I, E-12080 Castelló, Spain

M. Van Brussel and C. Buess-Hermann

Faculté de Sciences, Services de Chimie Analytique et Chimie des Interfaces, Université Libre de Bruxelles, CP 255, Boulevard du Triomphe, B-1050 Brussels, Belgium

P. Geerlings

Fakulteit Wetenschappen, Algemene Chemie, Vrije Universiteit Brussel, Pleinlaan 2, B-1050 Brussels, Belgium

Periodic DFT calculations are used to predict and investigate the adsorption behavior of molecular oxygen on Au, Au/Pt, and Pt surfaces. To obtain an array of pyramids containing surface atoms with the lowest possible coordination number, a nano-modified surface consisting of a symmetrically "modified" (100) surface was used. The effect of atom substitution (organized alloying) is investigated. The adsorption of molecular oxygen on a pure gold pyramid is exothermic by 0.77 eV for the end-on adsorption mode. In the case of a pure platinum pyramid, the end-on adsorption mode was found to dissociate; however, a side-on geometry was encountered with an energy of adsorption of 2.3 eV. This value is in line with the fact that the adsorption energy of small molecules does not vary much on Pt surfaces with different indices. Additionally, some geometrically related trends of the surface deformation in relation to its composition and after adsorption of molecular oxygen are highlighted.

Introduction

In contrast with gold as bulk material,[1] many experiments and recent applications prove the existence of a reactive form of gold. Nanometer-size gold particles on different oxide supports can act as catalysts even at or below room temperature.[2−4] Recently, mono- and dicarbonyls were observed on gold field emitter tips during interaction with CO gas at room temperature and in the presence of high electrostatic fields,[5] and the reduction of oxygen has been found to be kinetically more favorable on gold-modified platinum electrodes.[6]

The most likely first use for gold catalysts is for the removal of carbon monoxide impurities from the hydrogen feedstock streams used for fuel cells. Absence of carbon monoxide would enable fuel cells to run at lower temperatures and with improved efficiency.

Supported gold catalysts are also active in the water gas shift reaction used for producing hydrogen from carbon monoxide and water. Research has shown that gold supported on iron oxide (Au/α-Fe_2O_3) catalyst is more active at lower temperatures than both the α-Fe_2O_3 support and the mixed copper/zinc oxide (CuO/ZnO) catalyst currently used commercially. Gold nanoparticles exhibit high activity in low-temperature oxidation also on other metal oxides such as TiO_2, ZrO_2, Co_3O_4, and NiO.[4]

Besides the CO adsorption, the reduction of oxygen has found a variety of technological applications. In aqueous solutions, oxygen reduction is a multielectron reaction that may proceed according to two overall pathways: a direct four-electron reduction to water and a peroxide pathway that involves a two-electron reduction leading to peroxide as intermediate, which can undergo further reduction or decomposition.

The justification for developing gold catalyst technologies is not only based on their promising technical performance, but also on the relatively low stable price and greater availability of gold as compared to the platinum group metals.[7] The use of gold catalysts could therefore produce a welcome reduction in the capital cost of fuel cell installations. Other applications for gold in fuel cells are described and include its use as a corrosion resistant material and the incorporation of gold catalysts to provide useful improvements in electrode conductivity.

It is well known that the activity for oxygen reduction depends on the nature of the electrode used during the electroreduction, both in acidic and in alkaline media. The activity of platinum and gold is well documented in the literature.[8,9] Bulk platinum has the highest activity toward oxygen reduction, and the electroreduction involves four electrons leading to the formation of water as final product. On the other hand, bulk gold displays a poor activity for the same reaction and reduces oxygen to hydrogen peroxide, by a two-electron mechanism. However, information is lacking regarding the adsorption configuration of oxygen on these electrodes.

It was previously reported that a gold substrate can increase the activity of a platinum adlayer toward specific probe reactions, like the CO oxidation.[10] This observation was tentatively explained using a simple model in which the change in the CO binding energy is directly proportional to the shift of the d-band of the metal overlayer. According to this model, the
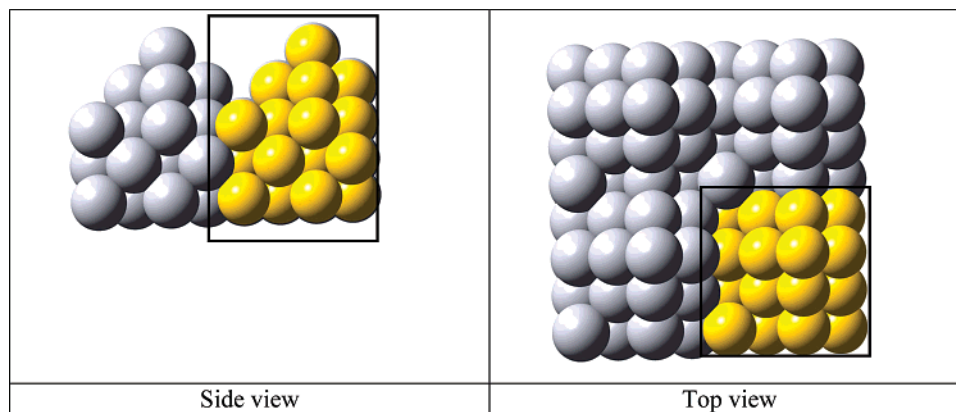

Figure 1. Super cell used in the case of the 29-atom cluster (super cell used in yellow).

increased activity of the Pt/Au system should be expected for other adsorbates and reactions. Indeed, recently, experimental data reported by us for oxygen reduction on platinum adlayer on gold[6,11] have shown an increase in activity for platinum particles grown on gold by an open-circuit deposition procedure called displacement deposition. An increase in activity toward oxygen reduction was reported for platinum modified gold electrodes with a specific gold/platinum ratio. In some cases, the activity was comparable to or higher than the activity of a bulk platinum electrode, although only small amounts of platinum were involved.

More specifically, the number of electrons involved in the electroreduction of oxygen on gold electrodes with Pt as surface modifier was found to be equal or close to four, even for limited amounts of platinum deposited on gold, both in acidic and in alkaline medium.[12] It is however noteworthy that all of the modified electrodes had residual gold atoms within the topmost atomic layers, regardless of the amount of platinum deposited onto the surface, as was revealed by our recent AES and XPS measurements.[6]

The activity of nanometer-size gold particles has been investigated experimentally and theoretically, and different reasons for this unexpected activity have been pointed out, such as the special role of the metal/support, the degree of co-ordinative unsaturation of the surface atoms, quantum size effects, tension, and recently the step density of the surface.[13] Not only small metal cluster changes the adsorption and reaction properties, but also alloying of the metals and monolayers or a few monolayers of one metal on top of another can have a quite significant influence on the adsorption[14,15] and reaction behavior of the metal itself.[16-18]

In this paper, the adsorption of oxygen is investigated on a gold surface modified on nanoscale to get an improved reactivity using DFT-based computational techniques in line with earlier theoretical work by the authors on heterogeneous catalysis or adsorption.[19-24] Besides the topology of the surface, the composition is also altered with the reactive platinum, that is, combining the topology and the alloying effect.

In line with the objectives of cluster science to discover highly stable systems to be used as building blocks for bulk materials, the surface used in this study simulating an array of gold tips or pyramids is comparable to similar clusters synthesized nowadays such as tetrahedra consisting of 20 gold atoms.[25]

The paper is organized as follows: Ab initio predictions are presented and discussed in relation with the experimental observations. In the first part, the changes in surface topology are discussed with respect to the Au/Pt composition followed by the analysis of the effect after molecular oxygen adsorption

on the top of a pyramid. Finally, the adsorption energies and the oxygen vibrational frequencies are investigated. Conclusions about the reactivity trend are drawn as well as suggestions to improve the reactivity of gold surface catalysts in relation toward molecular oxygen.

Computational Details

All geometry optimizations and minimizations of the total energy were performed using the Vienna Ab Initio Simulation Package (VASP) code.[26,27] In the periodic density functional theory framework used, the Kohn−Sham equations have been solved by means of the generalized gradient approximation proposed by Perdew and Wang[28,29] (GGA-PW91). The electron−ion interaction was described by the Projector Augmented-Wave method (PAW),[30,31] which allows the use of a low-energy cut off for the plane-wave basis set of 230 eV. For the Brillouin-zone integration, a $3 \times 3 \times 1$ Monkhorst-Pack special k-points grid has been used. A spin-unrestricted approach has been employed when molecular oxygen was adsorbed on the slab.

The relaxation of the atom positions and cell shape is performed via the action of a conjugate gradient optimization procedure. The slabs were fully optimized as well as the adsorbing oxygen molecule. A frequency calculation was achieved by calculation of the Hessian matrix followed by a diagonalization procedure to obtain the eigenmodes of the oxygen molecule.

The metal surface was modeled by super cells consisting of three bulk layers, two incomplete layers, and a vacuum, with starting cell dimensions of 8 Å × 8 Å × 20 Å, representing an intermediate value between Au an Pt. The application of periodic boundary conditions in all three Cartesian directions yields an infinite array of periodically repeated slabs separated by a region of vacuum of approximately 10Å. Optimization of the distances between the different atoms is allowed due to the variation of the cell shape (ISIF = 4 option in VASP). Although the volume is kept constant, the cell can expand in the *x* and *y* directions and shrink in the *z* direction. This procedure enables the optimization of the different bonds available in our model.

Two super cells, one with 29 and another with 32 atoms (see Figures 1 and 2), are considered, that is, constructed as layers of 1/4/8/88 and 1/4/9/99 (top/middle/base/support) gold atoms, respectively (see Figure 3). The different structures constructed were the following: pure or full Au (Au/Au/Au/AuAu) or Pt (Pt/Pt/Pt/PtPt) structures, Pt/Au/Au/AuAu, Au/Pt/Pt/PtPt, refer-ring to an Au pyramid (1 top, 4 middle, and 8 or 9 base atoms, and 2 layers of support) on a Pt base and opposite, Au/Au/Pt/AuAu, Pt/Au/Pt/PtPt, Pt/Pt/Au/PtPt, and Au/Au/Au/PtPt refer-
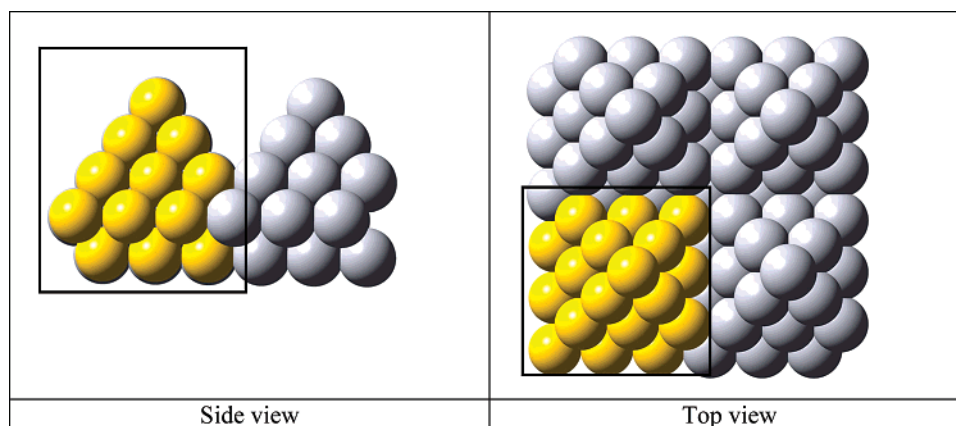
Figure 2. Super cell used in the case of the 32-atom cluster (super cell used in yellow).

ring to the layers of the pyramid substituted (top, middle, base, support) by Pt or Au on a Pt or Au support (see Figure 3).

Based on recent experimental findings in which oxygen binds stronger on low-coordinated Au atoms than on high-coordinated, such as on a sharp needle,[5,32] the slabs were constructed in such a way to simulate a gold tip or an array of nanoscale pyramids to simulate a gold surface with enhanced oxygen adsorption properties on one side and an unmodified (100) surface on the other side. Calculations for isolated atoms or molecules were performed in the same super cell arrangement as above.

Results and Discussion

(a) Calculation of Bulk Au and Bulk Pt. To test the accuracy of the computational approach, the lattice constant of bulk (FCC) gold and bulk (FCC) platinum was calculated by minimizing the system's total energy. The same energy cut off value was used for the plane wave expansion as in the slab calculations. The Brillouin-zone integration was performed on a Monkhorst-Pack $11 \times 11 \times 11$ k-point mesh. To evaluate the cohesive energy of the metals used (Au and Pt), a single atom in a cubic cell with 12 Å large sides was used to approximate an isolated atom. Its total energy was then calculated using the Γ-point in the Brillouin zone integration. The cohesive energy was obtained as the difference of a gold atom in bulk and the isolated atom. A lattice constant of 4.13 and 3.96 Å was obtained for Au and Pt, respectively. A cohesive energy of 3.02 and 5.51 eV was obtained for Au and Pt, respectively. These values are in fairly good agreement with those from experiments:[33] 4.08 Å and 3.81 eV for Au and 3.92 Å and 5.84 eV[34] for Pt, for the lattice parameter and cohesive energy, respectively. The surface energy (E^{surf}) of the surface is calculated using:

$$E^{surf} = E^{slab} - nE^{bulk}/[S_1/(S_1 + S_2) + S_2/(S_1 + S_2)] \quad (1)$$

where E^{slab} is the slab energy, E^{bulk} is the bulk energy, S_1 is the full accessible pyramid surface, that is, the pyramid faces and the available (100) surface, and S_2 is the bottom (100) surface.

This formula takes into account the fact that the slab contains two different surfaces S_1 and S_2 (included in a weight factor $S_x/(S_x + S_y)$, with x and y the different surfaces considered). For the pure Au system, the surface energy of the (100) surface is found to be 1.53 J/Å^2, which is also in good agreement with the experimental value of 1.41 J/m^2.[35] The pyramid surface energy using formula 1 is equal to 1.63 and 1.88 J/m^2 for the Au29 and the Au32 cluster, respectively. In comparison with the (100) surface, the modified surface is 15−30% less stable.
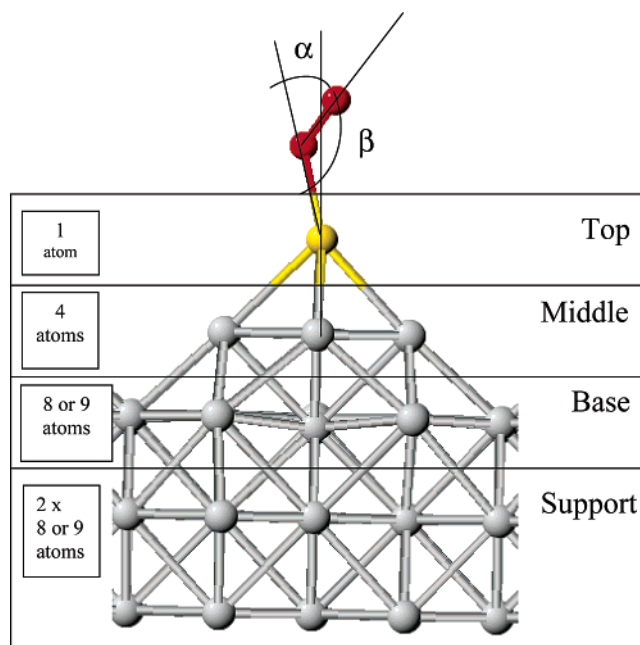

Figure 3. O_2 adsorbed on AuPtPtPt pyramid showing the angles α and β and the different parts of the layer (cluster) substituted by Au or Pt.

(b) Slab Geometries. To check the effect of atom substitution on the deformation and tension in the system, the geometrical parameters of the slabs are compared to experimental bulk results.

The Au pyramid height shrinks by 2.9% and 2.2% and the bottom layers expand by 2.3% and 3.6% in comparison with the bulk dimensions for the Au29 and Au32 cluster, respectively. The total volume shrinks by 4.3% and 1.7%, respectively. The horizontal Au−Au distance of both bottom layers does not change significantly, showing that the surface distortion has only an effect on the first two to three layers.

In the case of the Pt pyramid, the height shrinks by 10.5% and 9.1%, which is much more than in the Au case, leading to a total shrinkage of the pyramid volume of 11.8% and 7.8%, respectively. In contrast with gold, shrinkage of the bottom layers was found of 2.7% and 5.7% for Pt29 and Pt32, respectively. Comparing both Au and Pt pyramids, the Pt pyramid is 13% and 11% smaller, for the 29 and 32 structures, respectively. Interesting to note here is that platinum is much more sensitive on deformation and tension of the pyramid than gold.

The distance between two atoms in the support layers varies between 4.174 Å (Au−Au) and 3.849 Å (Pt−Pt) distance (in
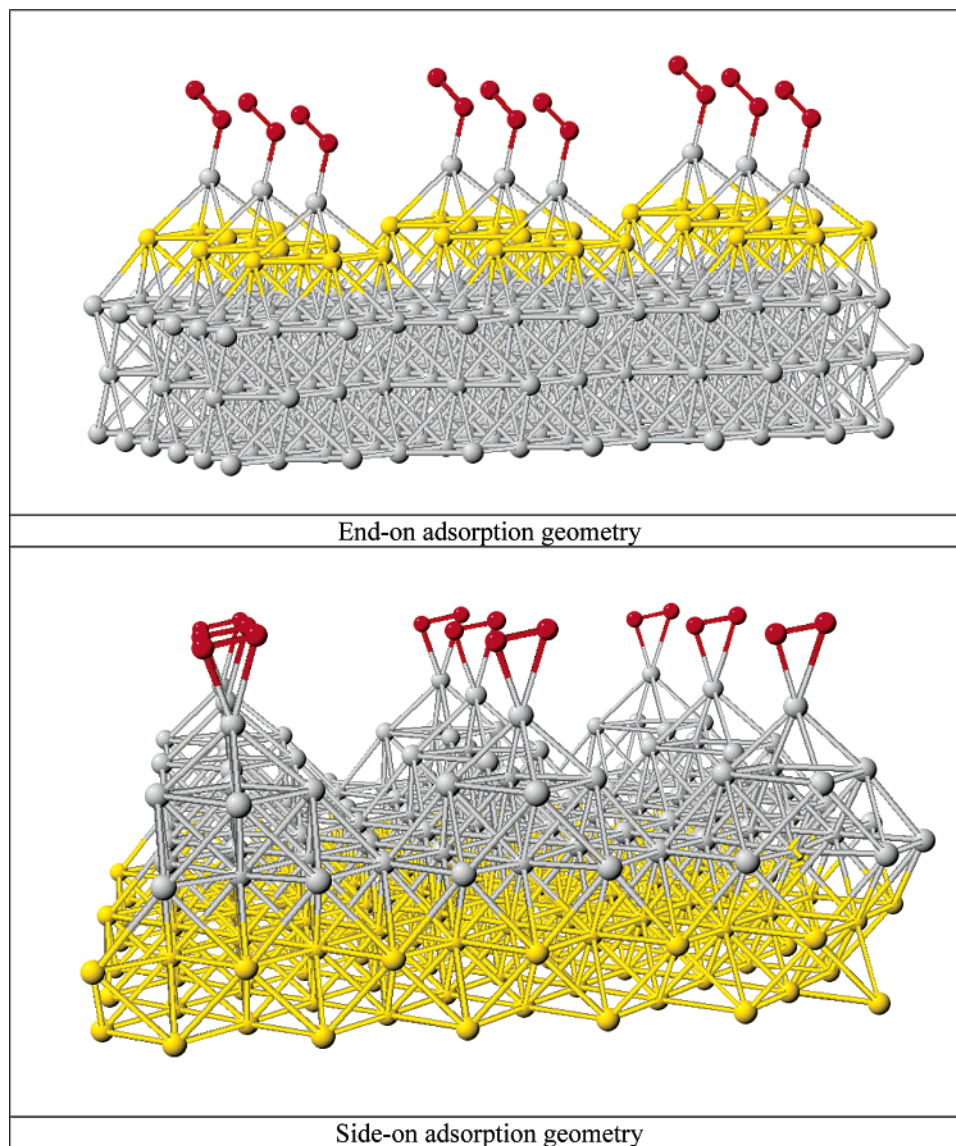
Study of Oxygen Adsorption on Gold Pyramids

J. Phys. Chem. B, Vol. 109, No. 16, 2005 **7627**

Figure 4. O_2 adsorption geometries on a pyramid considered in this study (end-on and side-on) ($3 \times 3 \times 1$ view) (red, oxygen; yellow, gold; and gray, platinum).

the z-direction). This distance shortens gradually when more Pt is inserted. In the support, Pt resists deformation the most, when the pyramid is substituted with Au atoms. In the opposite case (Au support and Pt pyramid), the deformation is 3% in length against 0.5% in the former case.

These results show that Pt is more resistant in the support layers than in the modified layers (tip). For Au, the opposite trend is found.

(c) Oxygen Adsorption Geometries. In this paper, we considered adsorption modes in contact only with the upper atom of the tip, that is, end-on and side-on adsorption geometries (see Figure 4). In the case of the end-on geometry, a tilted adsorption of the oxygen molecule on the top of the pyramid was encountered. The adsorption energy for the perpendicular geometry was approximately 0.2 eV less favorable. The side-on geometry shows the oxygen molecule parallel to the surface.

The Au pyramid volume of the 29 cluster is smaller than the 32 Au pyramid volume as was encountered in the pure Au and Pt cases without oxygen adsorption. The O_2 adsorption (end-on pattern) causes some drastic deformations to the geometry of the pyramid, such as the enlargement of the height of the

pyramid between 3% and 6%. The greatest enlargement is found for the Au/Pt/Pt/PtPt structure and the smallest for the Pt/Pt/Pt/AuAu structure, the Au/Pt/Pt/PtPt cluster having only an Au atom on top of a complete Pt pyramid and support (see Figure 3). The largest enlargements are found for the structures containing an Au base, as was the case for the support atoms (vide infra); in contrast, the structures containing a modifier of the other metal tend to resist deformation (Au/Au/Pt/AuAu and Pt/Pt/Au/PtPt), having the smallest deformations (1.6% and 3.2%). The tension introduced by the modifier behaves like strength in the structure. O_2 side-on adsorption on top shows the same trend as for the end-on modes; however, it influences the pyramid dimensions to a greater extent (7.8% for Au/Pt/Pt/PtPt29 and 0.25% Pt/Au/Au/AuAu).

The O—O bond distance does not change much between the different surfaces and adsorption modes: 1.36 ± 0.02 Å in the case of the end-on pattern, while for the side-on we encounter 1.40 ± 0.03 Å. The largest values are those for the interaction with a Pt atom or with a pyramid with Pt atoms. The oxygen bond length is longer, in agreement with a peroxoform. Those structures can be considered as potential precursors for oxygen

TABLE 1: Interaction Energies for Both Adsorption Geometries Considered (End-On and Side-On) on the Calculated 29-Atom Cluster (Values in eV)

system	full Au	Pt/Au/Au/AuAu	Au/Au/Au/PtPt	Au/Au/Pt/AuAu	Pt/Pt/Au/PtPt	Pt/Pt/Pt/AuAu	Au/Pt/Pt/PtPt	full Pt
end-on	−0.77	−1.02	−1.58	−0.81	−1.54	−0.56	−1.67	
side-on	−0.55	−0.89	−1.33	−0.66	−1.45	−0.39	−1.83	−2.31

dissociation (having similar O−O distances); however, a two-side adsorption should have a lower activation barrier.

The α angle (see Figure 3) is around 30° with an exception for Au/Pt/Pt/PtPt where an angle of −35° is found. The β angle is in all cases around 120°. The O-top distance is, as expected, shorter for an O−Pt interaction than for an O−Au interaction; the more Pt the pyramid holds the shorter the interaction distance is, which is in line with the fact that Pt is more reactive for O_2 than is Au. For the end-on pattern, it ranges from 1.94 to 2.22 Å; for the side-on pattern, it is slightly larger.

(d) Energies of Adsorption for Molecular Oxygen. Energies of adsorption ΔE_{ads} were calculated as:

$$\Delta E_{ads} = (E_{supercel} + E_{O_2}) - E_{supercell+O_2} \qquad (2)$$

where negative energies indicate exothermic adsorption (see Table 1).

First of all, adsorption of molecular oxygen was found to be favorable on a gold surface, which is a first indication that in contrast with adsorption on a (100) surface, where no adsorption is encountered at all, the shape (and thus the degree of coordination of the surface atoms) of the surface is of crucial importance.[36,37] Throughout the different adsorption modes considered on the gold containing pyramids, a relative high interaction energy was found. For the adsorption on a pure Au pyramid and on a Au pyramid supported on a Pt surface, interaction energies of approximately −0.6 to −0.8 eV and −0.9 to −1.0 eV were found, respectively. Because the energy differences and the trends between the interaction energies of the 29-atom and 32-atom clusters were quite identical, only the results for the 29-atom cluster are discussed.

Adsorption on a pure Pt pyramid (end-on pattern) turned out to be dissociative, as could be expected. On the other hand, an energy of adsorption of −2.3 eV is found for the side-on mode.

The absolute values suggest a quite strong interaction of Au. The adsorption energy of an O_2 molecule on a Au_2 molecule is −1.4 eV,[38] while on the stepped (211) Au surface a value of −0.12 eV[13] is found. Our values (see Table 1) of −0.77 and −0.55 eV show that these types of interactions are intermediate between Au clusters and a surface. This result confirms that the surface chosen increases the adsorption energy of a gold surface for molecular oxygen.

In the pure Pt case, the interaction energy could only be calculated for the side-on pattern (−2.3 eV). Comparing this value with the experimental adsorption energy on a Pt(111) surface (−2.1 eV), no tremendous increase is noticed. This result is in agreement with the findings of Lee et al.,[39] showing that the adsorption energies of small molecules vary little with the surface structure in the special case of platinum. Our results confirm this result in a broader extent because our surface has almost cluster properties as could be seen from the results for pure gold.

To study the effect of the degree of saturation on the adsorption trend, the side-on and end-on mode are more "appropriate" because the interaction occurs only with the top atom of the pyramid. However, other adsorption sites are available such as between two pyramids and on the side surface of a pyramid. Both adsorption sites were calculated and were found to be less favorable. Interesting to note here is that both

TABLE 2: O$_2$ Vibrational Frequency for the End-On Geometry on the Different Systems Considered (Values in cm^{-1})

system	freq (O−O)
full Au	1284
Pt/Au/Au/AuAu	1252
Au/Au/Au/PtPt	1246
Au/Au/Pt/AuAu	1212
Pt/Pt/Au/PtPt	1274
Pt/Pt/Pt/AuAu	1199
Au/Pt/Pt/PtPt	1223
full Pt	

the end-on and the side-on pattern adsorb relatively with the same adsorption energy throughout the whole range of Pt/Au concentration studied, but the trend is inverted when more Pt is introduced; that is, the side-on patterns is more favorable (0.16 eV) than the end-on pattern on a pure Pt pyramid or when the top is a Pt atom.

Looking at the adsorption trend in more detail, one can notice that when Au atoms are introduced the Pt pyramid becomes less reactive, even less reactive than a pure Au pyramid; however, the opposite trend is encountered for the gold top, to such an extent that placing a Pt atom on top of a pure Au pyramid is almost as reactive as a pure Pt pyramid (−1.7 vs −1.6 eV). Similar reactivity is encountered when the top is substituted with a Au and the four underlying atoms are substituted by Pt atoms (−1.5 eV). This interesting phenomenon suggests a specific interaction in the transition "zone" between Pt atoms and Au atoms.

(e) Calculation of the Oxygen Vibrational Frequencies. The adsorption geometries obtained were also analyzed by a vibrational frequency calculation of the O−O bond, achieved by calculation of the Hessian matrix followed by a diagonalization procedure to obtain the eigenmodes.

The calculation scheme was checked for molecular oxygen in the gas phase. The vibrational frequency obtained (1503 cm^{-1}) is in good agreement with the experimental value of 1580 cm^{-1}.[40] Interesting to note here is that this value is even closer to the experimental value than the B3LYP/LANL2DZ value of 1447 cm^{-1}.

The vibrational frequencies for the end-on pattern are presented in Table 2 and show the following trend (see Figure 5). One could expect a more linear relation between the interaction energy and the vibrational frequency. This result suggests a difference in type of interaction between O_2 and the nature of top atom of the pyramid. Indeed, looking at Figure 5, the frequency decreases when the molecule is better adsorbed if an Au atom is on the top of the pyramid, which is in line with our intuition. When the interaction increases, the oxygen bond weakens and the O−O vibrational frequency decreases. However, looking to the results for a Pt atom on top of the pyramid, one has to conclude the opposite. Looking at Figure 5, one can clearly distinguish both types of interaction. Even a third type of interaction is present, which cannot be organized in any of the groups, that is, the Au/Au/Au/PtPt structure. This is the structure giving the weakest interaction. This also shows that the influence of the support (i.e., 3 layers deep) is not affecting the interaction much.
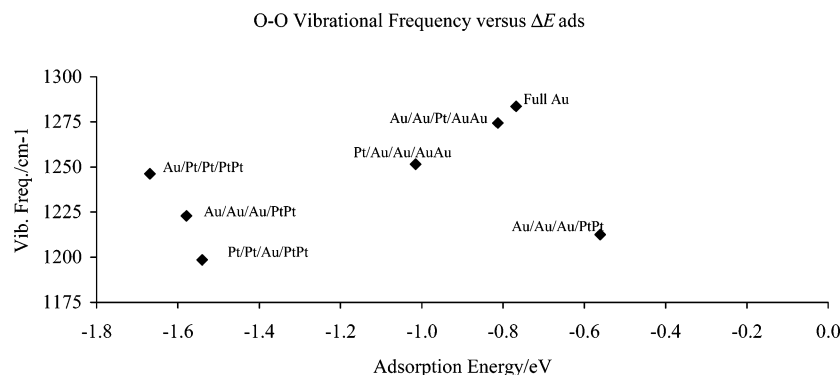
Study of Oxygen Adsorption on Gold Pyramids

J. Phys. Chem. B, Vol. 109, No. 16, 2005 **7629**

Figure 5. O_2 frequency trend linked to the pyramid composition.

Conclusions

Periodic DFT calculations were used to investigate the effect of modifiers combined with topological changes of a gold/platinum surface on the adsorption behavior of molecular oxygen.

It was found that Pt is more resistant to deformation in the pyramid than in the support layers, in contrast with Au, for which the opposite was concluded.

The end-on adsorption geometry of oxygen is found to be more stable than the side-on adsorption geometry. The pyramid enlarges after oxygen adsorption, and structures containing a modifier of the other metal tend to resist deformation (Au/Au/Pt/AuAu and Pt/Pt/Au/PtPt) having the smallest deformations. The tension introduced by the modifier behaves like strength in the structure.

The Au$-$O and the Pt$-$O distances were found to be in line with the interaction energy, that is, shorter distances for Pt than for Au. In all adsorption geometries studied, only small variations were encountered for the adsorption geometry as far as the O$-$O bond distance (21% enlargement in comparison with the free oxygen molecule) and the β angle is concerned (with T, a Au or Pt pyramid atom).

The results show clearly that modifying an Au surface in such a way that there are more unsaturated Au atoms available for adsorption gives a negative adsorption energy for oxygen. This improvement of the adsorption behavior of oxygen on a "modified" gold surface was not encountered for Pt surfaces. However, oxygen dissociated immediately on a Pt pyramid in end-on conformation, and the adsorption energy did not increase tremendously on our surfaces in comparison with the Pt(111) surface. This result confirms the fact that the interaction energy for small molecules does not vary considerably on different types of Pt surfaces.

Substituting Pt atoms for Au atoms improves the O_2 adsorption, however, only on specific positions. O_2 adsorption on a pyramid containing a gold atom on the top is less favorable than a complete golden pyramid. Remarkable is that the substitution of a Pt atom with an Au atom on top of the pyramid of a pure Pt system interacts with oxygen to the same extent as with a pure Pt pyramid.

The promoting effect of the gold substrate was found, insofar that the adsorption energies were -0.55, -1.8, and -2.31 eV on a bulk gold electrode, a platinum modified gold electrode, and a bulk platinum electrode, respectively. This shows that the adsorption and, therefore, the reduction of oxygen to water should be more favorable on a platinum modified gold electrode than on a bulk gold electrode. If the bond length was in this case also quite different, then a dissociative precursor state might be possible explaining why, on gold, no chemical breakdown

occurs and the reduction follows a two-electron pathway, while on a platinum modified gold electrode, the dissociation of the weakened adsorbed oxygen leads to a four-electron reduction to water.

Interestingly, while it is quite clear that the presence of a platinum atom on top of a gold pyramid increases the adsorption energy, the amount of platinum in the pyramid plays a significant role. Indeed, the adsorption energy of oxygen on a full platinum pyramid on top of a gold slab is higher than the adsorption energy on a single platinum atom at the apex, both for the side-on adsorption configuration and for the end-on configuration. This observation is in line with experimental results reported earlier for oxygen reduction, which showed that the electrocatalytic activity was directly related to the amount of platinum present on the gold surface.[6,11] It should therefore be possible, soon, to predict the optimal composition and configuration of a platinum modified gold electrode to take the most advantage from the promoting effect of the gold substrate.

Some future developments on the electronic structure of the alloying and topological changes on the nanoscale of the surfaces are in progress. This would enable us to investigate the density of states and the spin density of the system and in particular the electroreduction of oxygen.

References and Notes

(1) Hammer, B.; Nørskov, J. K. *Nature* **1995**, *376*, 238.

(2) Haruta, M. *Catal. Today* **1997**, *36*, 153.

(3) Valden, M.; Lai, X.; Goodman, D. W. *Science* **1998**, *281*, 1647.

(4) Grünwaldt, J. D.; Kiener, C.; Wögerbauer, C.; Baiker, A. *J. Catal.* **1999**, *181*, 223.

(5) Chai, T.-D.; Visart de Bocarmé, T.; Kruse, N.; Wang, R. L. C.; Kreuzer, J. *J. Chem. Phys.* **2003**, *119*, 12605.

(6) Van Brussel, M.; Kokkinidis, G.; Hubin, A.; Buess-Herman, C. *Electrochim. Acta* **2003**, *48*, 3909.

(7) Cameron, D.; Holliday, R.; Thompson, D. *J. Power Sources* **2003**, *118*, 298.

(8) Adzic, R. R. Recent advances in the kinetics of oxygen reduction. In *Electrocatalysis*; Lipkowski, J., Ross, P. N., Eds.; Wiley$-$VCH: New York, 1998; p 197.

(9) Markovic, N. M.; Schmidt, T. J.; Stamenkowic, V.; Ross, P. N. *Fuel Cells* **2001**, *1*, 105.

(10) Pedersen, M. Ø.; Helveg, S.; Ruban, A.; Stensgaard, I.; lægsgaard, E.; Nørskov, J. K.; Besenbacher, F. *Surf. Sci.* **1999**, *426*, 395.

(11) Van Brussel, M.; Kokkinidis, G.; Vandendael, I.; Buess-Herman, C. *Electrochem. Commun.* **2002**, *4*, 808.

(12) Brankovic, S. R.; Wang, J. X.; Adzic, R. R. *Surf. Sci.* **2001**, *474*, L173.

(13) Mavrikakis, M.; Stoltze, P.; Nørskov, J. K. *Catal. Lett.* **2000**, *64*, 101.

(14) Rodriguez, J. A.; Goodman, D. W. *Science* **1992**, 897.

(15) Rodriguez, J. A. *Surf. Sci. Rep.* **1996**, *24*, 223.

(16) Larsen, J. H.; Chorkendorff, I. *Surf. Sci.* **1998**, *405*, 62.

(17) Filhol, J. S.; Simon, D.; Sautet, P. *J. Am. Chem. Soc.* **2004**, *126*, 3228.

(18) Piccolo, L.; Loffreda, D.; Aires, F. J. C. S.; Deranlot, C.; Jugnet, Y.; Sautet, P.; Bertoloni, J. C. *Surf. Sci.* **2004**, *566*, 995.

(19) Vos, A. M.; Schoonheydt, R. A.; De Proft, F.; Geerlings, P. *J. Catal.* **2003**, *220*, 333.

(20) Vos, A. M.; Schoonheydt, R. A.; De Proft, F.; Geerlings, P. *J. Phys. Chem. B* **2003**, *107*, 2001.

(21) Vos, A. M.; Nulens, K. H. L.; De Proft, F.; Schoonheydt, R. A.; Geerlings, P. *J. Phys. Chem. B* **2002**, *106*, 2026.

(22) Tielens, F.; Saeys, M.; Tourwé, E.; Marin, G. B.; Hubin, A.; Geerlings, P. *J. Phys. Chem. A* **2002**, *106*, 1450.

(23) Tielens, F.; Denayer, J.; Daems, I.; Baron, G. V.; Mortier, W. J.; Geerlings, P. *J. Phys. Chem. B* **2003**, *107*, 11065.

(24) Tielens, F.; Geerlings, P. *J. Mol. Catal. A* **2001**, *166*, 175.

(25) Zhang, H.-F.; Stender, M.; Zhang, R.; Wang, C.; Li, J.; Wang, L.-S. *J. Phys. Chem. B* **2004**, *108*, 12259.

(26) Kresse, G.; Hafner, J. *Phys. Rev. B* **1994**, *49*, 14251.

(27) Kresse, G.; Furthmuller, J. *Comput. Mater. Sci.* **1996**, *6*, 15.

(28) Perdew, J. P.; Chevary, J. A.; Vosko, S. H.; Jackson, K. A.; Pederson, M. R.; Singh, D. J.; Fiolhais, C. *Phys. Rev. B* **1992**, *46*, 6671.

(29) Perdew, J. P.; Wang, Y. *Phys. Rev. B* **1992**, *45*, 13244.

(30) Kresse, G.; Joubert, J. *Phys. Rev. B* **1999**, *59*, 1758.

(31) Blöchl, P. E. *Phys. Rev. B* **1994**, *50*, 17953.

(32) Bar, T.; Visart de Bocarmé, T.; Nieuwenhuys, B. E.; Kruse, N. *Catal. Lett.* **2001**, *74*, 127.

(33) Kittel, C. *Introduction to Solid State Physics*; Wiley: New York, 1986.

(34) Häberlen, O. D.; Chung, S.-C.; Stener, M.; Rösch, N. *J. Chem. Phys.* **1997**, *106*, 5189.

(35) Cosandey, F.; Madey, T. E. *Surf. Rev. Lett.* **2001**, *8*, 73.

(36) Bond, G. C. *Catal. Today* **2002**, *72*, 5.

(37) Tanaka, K.; Tamaru, K. *J. Catal.* **1963**, *2*, 366.

(38) Mills, G.; Gordon, M. S.; Metiu, H. *Chem. Phys. Lett.* **2002**, *359*, 493.

(39) Lee, W. T.; Ford, L.; Blowers, P.; Nigg, H. L.; Masel, R. I. *Surf. Sci.* **1998**, *416*, 141.

(40) Huber, K. P.; Herzberg, G. *Molecular Spectra and Molecular Structure. IV Constants of Diatomic Molecules*; Van Nostrand Reinhold Co.: New York, 1979.